Electronic Supplementary Material: Theoretical X-Ray Absorption Spectroscopy Database Analysis for Oxidized 2D Carbon Nanomaterials

Fabian Weber[a,b], Jian Ren[a,c], Tristan Petit[a], Annika Bande[a]

[a] Institute of Methods for Material Development, Helmholtz-Zentrum Berlin für Materialien und Energie GmbH, Albert-Einstein-Str. 15, 12489 Berlin, Germany.

[b] Department of Chemistry and Biochemistry, Freie Universität Berlin, Takustr. 3, 14195 Berlin, Germany.

[c] Department of Physics, Freie Universität Berlin, Arnimallee 14, 14195 Berlin, Germany.

A. CONJUGATION EFFECTS

As mentioned in the main article, the local uniqueness of XA excitations may break down when the virtual orbital space is strongy affected by conjugation effects, like in chromophores. To probe how strongly these effects impact the theoretical individual-atom spectra and what implications that has on the database, we discuss the theoretical total XA spectra of three small, linear π-conjugated molecules (cf. Fig. 1). Here, we shall compare the different positions of carbon atoms along the chain of conjugated π-bonds for all three model structures.

In the uppermost panel of Fig. S1, the individual-atom XA spectra of the ending CH_2 of the three structures are compared. One can see that in all three structures the first signal which belongs to the σ^*(C=C) transition is at the same energetic position when using a carbonyl group (blue), as well as for the pristine butadiene (black). The signal for R= COOH (red) is shifted to higher energies by about 0.3 eV compared to the other two. This behaviour reproduces the expectation that a carboxyl group shows an overall greater effect on the electronic structure in a π-conjugated chain of carbon atoms. The shift to higher energies is even more pronounced for the σ^*(C-H) transition around 289.0 eV. Here, the carbonyl and carboxyl are shifted to higher energies by 0.6 eV and 0.9 eV, respectively. This behaviour generally continues along the other positions of the conjugated chain, while increasing in magnitude the closer the individual atom is to the rest R.

As expected, the conjugation effects present a challenge to the local excitation approach. However, one should keep in mind that by applying a database indexing scheme one is

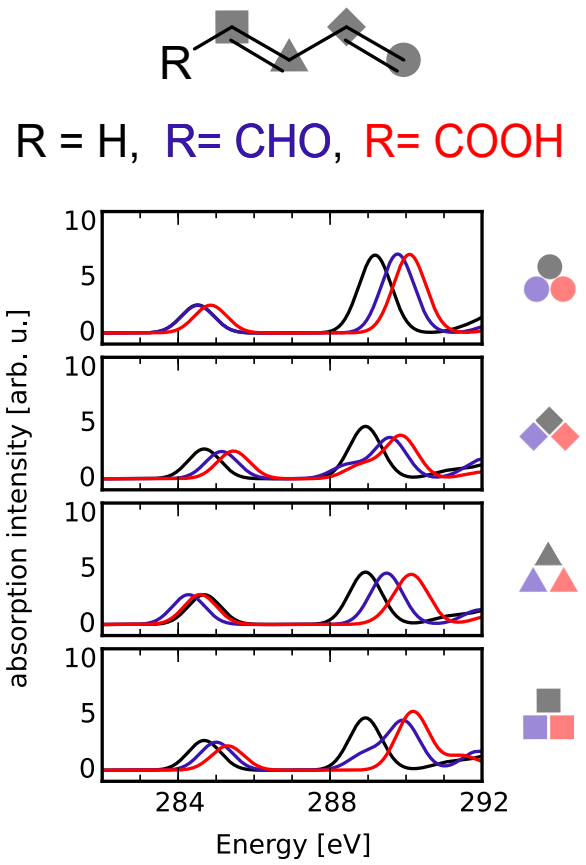

FIG. S 1. Comparison of local conjugation effects in three different molecules (color online), on four different carbon atoms. Each panel shows one of the four highlighted positions in all three structures.

able to distinguish the most affected atoms from each other efficiently. Within the reduced NNN indexing that was applied throughout the present article, one may fully distinguish the individual-atom spectra of the carbon atoms closest to the rest R (marked with quadrats in Fig. S1), since they would be indexed as connector atoms to the carbonyl and carboxyl groups, giving rise to the "C-CHO" and "C-COOH" functionalities. If the full NNN indexing was applied, also the next atom (triangles) would be fully distinguished since they would contain one of the C-COOH, C-CHO or CH_2 atoms in their own nearest neighbour list. Therefore, despite the presence of conjugation effects, the presented method is capable of including also non-local excitation effects by increasing the indexing radius.

B. ANALYSIS OF GROUP XA SPECTRA

In the following, the eighteen different mean group XA spectra are analyzed with respect to the types of transitions for the strongest features. We also include a comparison with experimental data in tabular form. The mean group XA spectra were obtained from averaging over each respective NNN-distinguishable group among all **C** and **CC** model structures. Note that no normalization of spectra is performed, but rather each spectrum was divided by the number of carbon atoms in that group. The assignment of peaks was performed by evaluating the virtual Kohn-Sham orbital space included in the transition in a local way.

B.1 Carbon scaffold

We start the analysis by looking at the XA group spectra of three types of aromatic carbon atoms that may be distinguished in the NNN indexing (see Fig. S2). Firstly, one can see that the basal C, bridge C and edge CH groups display a signal around 285.0 eV, which is in the expected range for π^*(C=C) transitions (*cf.* Tab. 2 of the main article). Furthermore, a strong signal around 289.0 eV is prominent for the edge CH, which, based on the virtual KSOs involved in the transition, may be attributed to transitions from the C 1s orbital into σ^*(C−H) orbitals. The energetic position of the σ^*(C-C) transition of the bridge C position seems to be heavily influenced by conjugation effects, as discussed in the previous section A.

Besides that the carbon scaffold also includes the hydrogenated groups basal CH, bridge CH and edge CH_2, the spectra of which are shown in Fig. S3. Firstly, one notices the absence of the strong π^*(C=C) transition, since these groups only contain sp^3 hybridized carbon atoms. All three groups also show two σ^*(C−H) transitions at similar energies of 289.2 eV and 291.6 eV. Note that the occurrence of two peaks in the cumulated group picture does not imply the actual existence of two peaks in a single individual atom spectrum, but rather that the multitude of spectra would contain either one type of σ^*(C−H) transition or the other. In other words, by grouping the spectra together with respect to the NNN indexing scheme in this first approximation, one can end up with both a number of secondary peaks or a general broadening of the signals due to energy shifts in the target virtual orbitals of the excitation. Although this may seem like a drawback at first, it may help studying the

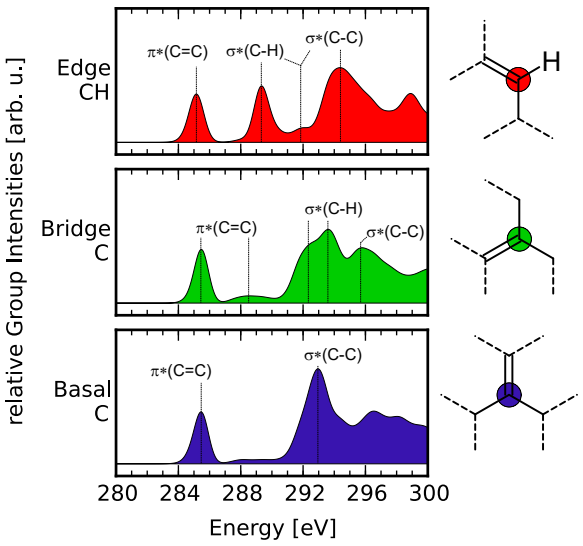

FIG. S 2. Group XA spectra of three different aromatic carbon atoms.

case of non-ordered and defectuous materials more realistically, since we may distinguish which signals are influenced by this shifting more than others and identify the transition characteristic of the secondary peaks. Also, this averages out some of the errors made by deprecating the indexing radius.

Finally, since there are no conjugation effects expected for the sp^3 hybridized atoms, the energy for the σ^*(C−C) transition is almost identically found around 294.8 eV.

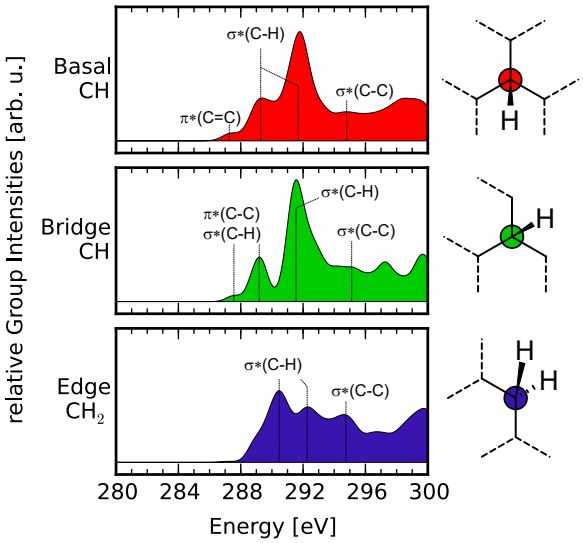

FIG. S 3. Group XA spectra of three different hydrogenated carbon atoms.

TAB. S I. List of transition types for unfunctionalized carbon atoms.

Group	**Assignment**	**Energy (theo.) [eV]**	**Energy (exp.) [eV]**
basal CH	π^*(C−C)	287.3	284.3 - 286.7[1–5]
	σ^*(C−H)	289.3	286.0 - 292.0[3,4]
	σ^*(C−H)	291.8	286.0 - 292.0[3,4]
	σ^*(C−C)	294.8	289.0 - 295.6[1,5]
bridge CH	π^*(C−C)	287.5	284.3 - 286.7[1–5]
	σ^*(C−H)	289.2	286.0 - 292.0[3,4]
	σ^*(C−H)	291.6	286.0 - 292.0[3,4]
	σ^*(C−C)	295.0	289.0 - 295.6[1,5]
edge CH_2	σ^*(C−H)	290.5	286.0 - 292.0[3,4]
	σ^*(C−H)	292.3	286.0 - 292.0[3,4]
	σ^*(C−C)	294.6	289.0 - 295.6[1,5]
edge CH	π^*(C=C)	285.2	284.3 - 286.7[1–5]
	σ^*(C−H)	289.4	286.0 - 292.0[3,4]
	σ^*(C−H)	292.1	286.0 - 292.0[3,4]
	σ^*(C−C)	292.1	289.0 - 295.6[1,5]
	σ^*(C−C)	294.4	289.0 - 295.6[1,5]
bridge C	$1\pi^*$(C=C)	285.5	284.3 - 286.7[1–5]
	$2\pi^*$(C=C)	288.5	288.6 - 289.1[3,5]
	σ^*(C−H)	292.4	286.0 - 292.0[3,4]
	σ^*(C−H)	293.6	286.0 - 292.0[3,4]
	σ^*(C−C)	295.8	289.0 - 295.6[1,5]
basal C	π^*(C=C)	285.5	284.3 - 286.7[1–5]
	σ^*(C−C)	293.0	289.0 - 295.6[1,5]

B.2 Epoxy groups

Next, we shall discuss the spectra related to the three positions basal, bridge and edge of epoxidized carbon atoms (*cf.* Tab. 3 of the main article). Take note that in case of the edge position the carbon atom is saturated by an additional hydrogen atom. All three groups show a σ^*(C−O) transition around 287.5 eV, where the p_z orbitals of the two epoxy-bound carbons form antibonding Kohn-Sham orbitals (KSO) with the oxygen's p orbital.

For the bridge as well as edge position one finds a signal roughly around 290 eV that can be attributed to σ^*(C−H) transitions. While the edge position is directly connected to a hydrogen atom, the bridge position undergoes this transition via conjugation effects. Furthermore, we find a strong transition of π^*(C−C) character around 292 eV for the basal and bridge positions that is broadened for the bridge position and only occuring as a shoulder

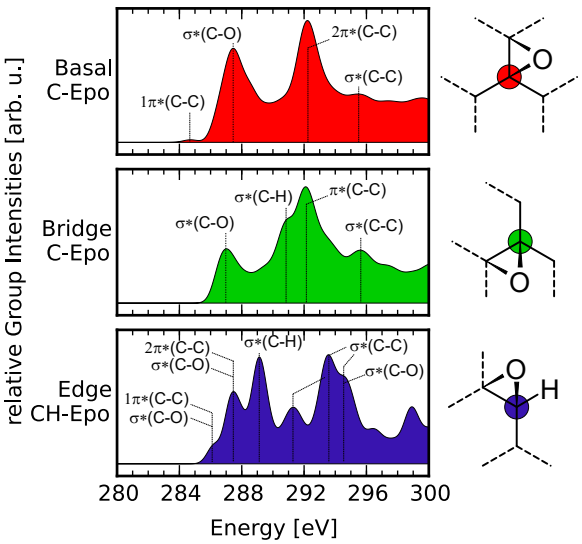

FIG. S 4. Group XA spectra of three different epoxidized carbon atoms.

in the basal position. The edge position seems not to be able to to undergo this transition, which may be due to the fact that it is the only of the three groups where the C-O-C bonding plane is not intersecting the graphene sheet perpendicularly, but may rather tilted to it. For the bridge and basal position this transition involves both virtual orbitals of π^*(C—C) as well as σ^*(C—O) nature, which is in qualitative agreement with NEXAFS studies of different epoxy-polymers.[4]

B.3 Hydroxyl groups

In Fig. S5, we discuss four different types of hydroxyl-functionalized carbon atoms. First of all, the sp^2 hybridized phenolic edge C-OH group is the only group among the four types that shows a π^*(C=C) transition around 285.4 eV. Interestingly, despite being sp^3 hybridized, the basal as well as bridge positions also show a weak transition of π^*(C—C) nature, because of hyperconjugation of the sp^3-type orbitals with the surrounding π^* network.

Besides that, all of the hydroxyl carbon group spectra additionally show a more or less pronounced σ^*(O—H) transition around 289 eV for the bridge and basal position and around 290 eV for the edge position. For both the basal as well as bridge positions, the signal's intensity is enhanced by energetically degenerate $2\pi^*$(C—C) transitions. For the edge position, both the phenolic and hydrogenated species' signals are coinciding with σ^*(C—O) excitations. Since the C-O and O-H bonds are relatively flexible, the broadening of the sig-

TAB. S II. List of transition types for epoxidized carbon atoms.

Group	**Assignment**	**Energy (theo.) [eV]**	**Energy (exp.) [eV]**
basal C-Epo	$1\pi^*$(C−C)	284.7	284.3 - 286.7[1–5]
	σ^*(C−O)	287.5	287.9 - 294.5[1,2,5,6]
	$2\pi^*$(C−C)	292.2	288.6 - 289.1[3,5]
	σ^*(C−C)	295.5	289.0 - 295.6[1,5]
bridge C-Epo	σ^*(C−O)	287.0	287.9 - 294.5[1,2,5,6]
	σ^*(C−H)	291.0	284.3 - 286.7[1–5]
	π^*(C−C)	292.1	286.0 - 292.0[3,4]
	σ^*(C−C)	295.6	289.0 - 295.6[1,5]
edge CH-Epo	$1\pi^*$(C−C)	286.2	284.3 - 286.7[1–5]
	σ^*(C−O)	286.2	287.9 - 294.5[1,2,5,6]
	$2\pi^*$(C−C)	287.5	288.6 - 289.1[3,5]
	σ^*(C−O)	287.5	287.9 - 294.5[1,2,5,6]
	σ^*(C−H)	289.1	286.0 - 292.0[3,4]
	σ^*(C−C)	291.3	289.0 - 295.6[1,5]
	σ^*(C−C)	293.6	289.0 - 295.6[1,5]
	σ^*(C−C)	294.4	289.0 - 295.6[1,5]
	σ^*(C−O)	294.4	287.9 - 294.5[1,2,5,6]

nals is strongly related to different angles and distances among the p orbital of the excited carbon atom and the target σ^*(O−H) orbital.

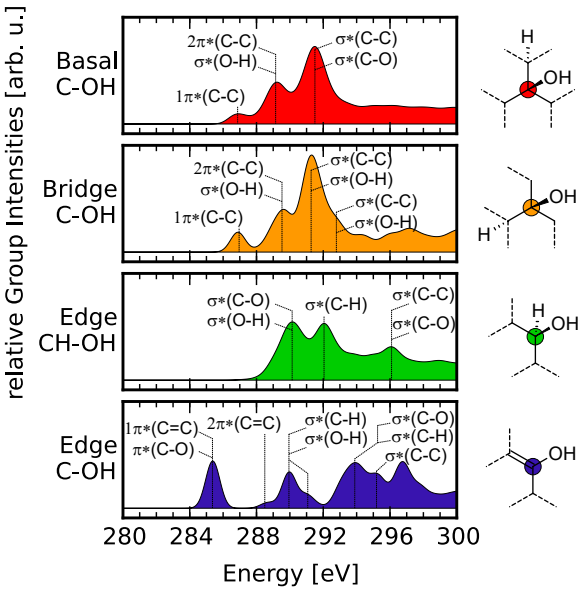

FIG. S 5. Group XA spectra of four different hydroxylated carbon atoms.

Finally, one finds the σ^*(C−C) transition at around 291.5 eV for both the basal as well

TAB. S III. List of transition types for hydroxylized carbon atoms.

Group	**Assignment**	**Energy (theo.) [eV]**	**Energy (exp.) [eV]**
basal C-OH	$1\pi^*$(C−C)	286.9	284.3 - 286.7[1–5]
	$2\pi^*$(C−C)	289.2	288.6 - 289.1[3,5]
	σ^*(O−H)	289.2	287.0 - 288.3[1,5]
	σ^*(C−C)	291.5	289.0 - 295.6[1,5]
	σ^*(C−O)	291.5	287.9 - 294.5[1,2,5,6]
bridge C-OH	$1\pi^*$(C−C)	286.9	284.3 - 286.7[1–5]
	$2\pi^*$(C−C)	289.6	288.6 - 289.1[3,5]
	σ^*(O−H)	289.6	287.0 - 288.3[1,5]
	σ^*(C−C)	291.3	289.0 - 295.6[1,5]
	σ^*(O−H)	291.3	287.0 - 288.3[1,5]
	σ^*(C−C)	292.8	289.0 - 295.6[1,5]
	σ^*(C−O)	292.8	287.9 - 294.5[1,2,5,6]
edge CH-OH	σ^*(C−O)	290.2	287.9 - 294.5[1,2,5,6]
	σ^*(O−H)	290.2	287.0 - 288.3[1,5]
	σ^*(C−H)	292.1	286.0 - 292.0[3,4]
	σ^*(C−C)	296.1	289.0 - 295.6[1,5]
	σ^*(C−O)	296.1	287.9 - 294.5[1,2,5,6]
edge C-OH	$1\pi^*$(C=C)	285.4	284.3 - 286.7[1–5]
	π^*(C−O)	285.4	288.0 - 290.9[1,2,5,6]
	$2\pi^*$(C−C)	288.7	288.6 - 289.1[3,5]
	σ^*(C−H)	290.0	286.0 - 292.0[3,4]
	σ^*(O−H)	290.0	287.0 - 288.3[1,5]
	σ^*(C−H)	291.1	286.0 - 292.0[3,4]
	σ^*(O−H)	291.1	287.0 - 288.3[1,5]
	σ^*(C−O)	293.9	287.9 - 294.5[1,2,5,6]
	σ^*(C−H)	293.9	286.0 - 292.0[3,4]
	σ^*(C−C)	295.1	289.0 - 295.6[1,5]

as the bridge position, while the signal with this character is found only above 295.0 eV for the edge position. The intense signal at 292.1 eV in the edge CH-OH group belongs to a σ^*(C−H) transition that is unique for the hydrogenated edge carbon atoms.

B.4 Higher oxidized groups

Lastly, in Fig. S6 the carbonylic, carboxylic and ketone groups shall be discussed together with the carbon atoms that connect them to the GO scaffold (i.e. edge C-COOH and edge C-CHO). Please note that almost all transitions in these groups are coincident with other

transitions due to strong conjugation of the π-system (cf. Tab. 5 of the main article). This is also reflected by the fact that each of the CHO or COOH group's spectra is very similar to the spectrum of the respective connector carbon atom.

At low excitation energies, one first finds a signal for π^*(C−C) for all five groups. The carboxyl, carbonyl and ketone atom exhibit this transition around 284 eV, while the edge connector C-CHO and C-COOH atoms show this transition at 285 eV. The reason for the difference in excitation energies can be explained by the strongly electronegative oxygen-atoms that facilitate drawing excited electrons into the antibonding π^*(C−C) system they are conjugated with.

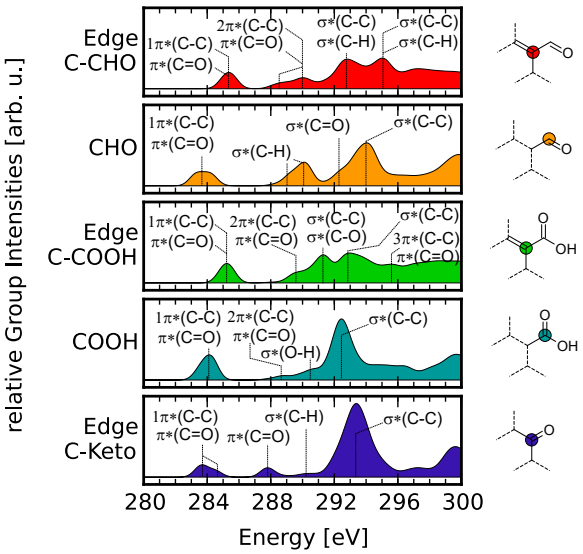

FIG. S 6. Group XA spectra of higher oxidized carbon atoms and the respective edge atoms connecting to those.

Next in energetic ordering one finds a similar spectral signature for all four groups besides the ketone that is composed of a small shoulder followed by a larger, broad signal. In case of the edge C-CHO group (top panel), the two peaks are caused by two different cases of coupled π^*(C−C) and π^*(C=O) transitions. The first signal centred at 288.5 eV is found only in model structures where the π system is not greatly disturbed by other functional groups in the vicinity of the edge C-CHO carbon (marked with a superscript *a* in Tab. 5 of the main article), while in the other scenario the transition is further influenced through conjugation with even farther functional groups (marked with a superscript *b* in Tab. 5 of the main article). This finding shows that increasing the indexing radius is important for

the carbonyl and carboxyl group.

For the CHO group XAS the same issue arises, since there the first peak at 289.1 eV is caused by σ^*(C−H) transitions in the undisturbed case, while the second, more intense signal at 290.2 has the same transition characteristic in the more functionalized model structures. Again, the relative intensities are only governed by the number of occurrences.

The COOH related groups, however, show no such strong dependency on the farther away groups than the CHO related species. For the edge C-COOH, the first of the two signals at 289.7 eV corresponds to π^*(C−C) and π^*(C=O) transitions again, while the second signal at 291.3 eV is given by the σ^*-symmetric transition for the same two atoms. Finally, the carboxyl atoms themselves show the same coupled π^*(C−C) /π^*(C=O) transition at 288.6 eV and an σ^*(O−H) transition at 290.7 eV. We believe that the COOH related species are not influenced by the environment as much as the CHO ones, because the local virtual space into which electrons are excited may be significantly more locally confined due to two oxygen atoms attracting the electron density.

Finally, the ketone carbon group (bottom) shows only a π^*(C=O) transition around 287.8 eV and a σ^*(C−H) transition in this whole region.

TAB. S IV. List of transition types for higher oxidized carbon atoms.

Group	**Assignment**	**Energy (theo.) [eV]**	**Energy (exp.) [eV]**
edge	$1\pi^*$(C−C)	285.4	284.3 - 286.7[1–5]
C-CHO	$1\pi^*$(C=O)	285.4	288.0 - 290.9[1,2,5,7,8]
	$2\pi^*$(C−C)[a]	288.8	288.6 - 289.1[3,5]
	$2\pi^*$(C=O)[a]	288.8	288.0 - 290.9[1,2,5,7,8]
	$2\pi^*$(C−C)[b]	290.0	288.6 - 289.1[3,5]
	$2\pi^*$(C=O)[b]	290.0	288.0 - 290.9[1,2,5,7,8]
	σ^*(C−C)	292.8	289.0 - 295.6[1,5]
	σ^*(C−H)	292.8	286.0 - 292.0[3,4]
	σ^*(C−C)	295.0	289.0 - 295.6[1,5]
	σ^*(C=O)	295.0	287.9 - 294.5[1,2,5,6]
CHO	$1\pi^*$(C−C)	283.7	284.3 - 286.7[1–5]
	$1\pi^*$(C=O)	283.7	288.0 - 290.9[1,2,5,7,8]
	σ^*(C−H)[a]	289.1	286.0 - 292.0[3,4]
	σ^*(C−H)[b]	290.1	286.0 - 292.0[3,4]
	σ^*(C=O)[b]	292.5	287.9 - 294.5[1,2,5,6]
	σ^*(C=O)[a]	292.9	287.9 - 294.5[1,2,5,6]
	σ^*(C−C)	294.0	289.0 - 295.6[1,5]
edge	$1\pi^*$(C−C)	285.2	284.3 - 286.7[1–5]
C-COOH	$2\pi^*$(C=O)	285.2	288.0 - 290.9[1,2,5,7,8]
	$2\pi^*$(C−C)	289.7	288.6 - 289.1[3,5]
	$3\pi^*$(C=O)	289.7	288.0 - 290.9[1,2,5,7,8]
	σ^*(C−C)	291.3	289.0 - 295.6[1,5]
	σ^*(C−O)	291.3	287.9 - 294.5[1,2,5,6]
	σ^*(C−C)	293.0	289.0 - 295.6[1,5]
	σ^*(O−H)	293.5	287.0 - 288.3[1,5]
	$3\pi^*$(C−C)[b]	295.6	294.0[3]
	$4\pi^*$(C=O)[b]	295.6	287.9 - 294.5[1,2,5,6]
COOH	$1\pi^*$(C−C)	284.1	284.3 - 286.7[1–5]
	$1\pi^*$(C=O)	284.1	288.0 - 290.9[1,2,5,7,8]
	$2\pi^*$(C−C)	288.9	288.6 - 289.1[3,5]
	$2\pi^*$(C=O)	288.9	288.0 - 290.9[1,2,5,7,8]
	σ^*(O−H)	290.6	287.0 - 288.3[1,5]
	σ^*(C−C)	292.5	289.0 - 295.6[1,5]
	σ^*(C−O)	296.2	287.9 - 294.5[1,2,5,6]
edge	π^*(C−C)	283.7	284.3 - 286.7[1–5]
C-Keto	$1\pi^*$(C=O)	284.5	288.0 - 290.9[1,2,5,7,8]
	$2\pi^*$(C=O)	287.8	288.0 - 290.9[1,2,5,7,8]
	σ^*(C−H)	290.5	286.0 - 292.0[3,4]
	σ^*(C−C)	293.4	289.0 - 295.6[1,5]

C. COMPOSITION OF DATABASE STRUCTURES

This section comprises all **C** and **CC** structures of the model molecules accompanied with their explicit theoretical total XA spectra and database compositions, similar to the analysis performed in Section "Comparison with explicit theoretical spectra" of the main article. The names accompanying the shown structures are the ones used for the .xyz-files, respectively. In the commentary line of the .xyz files the total energy is given.

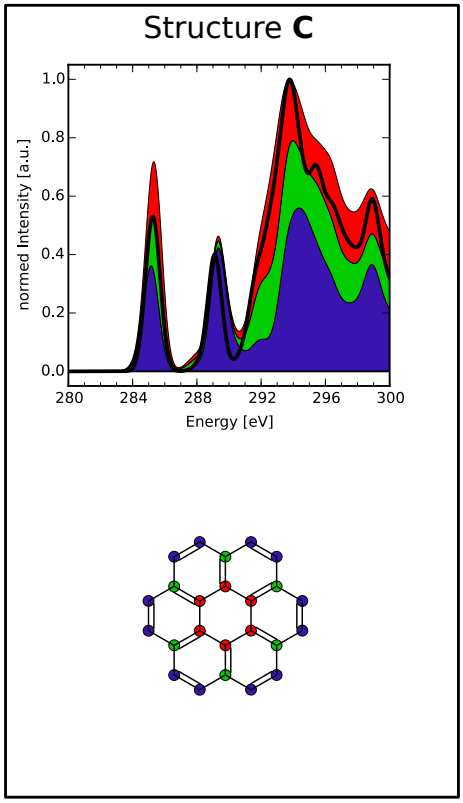

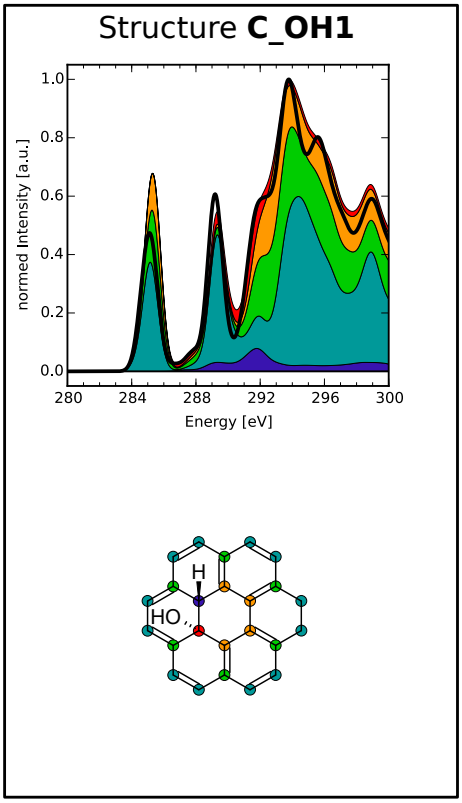

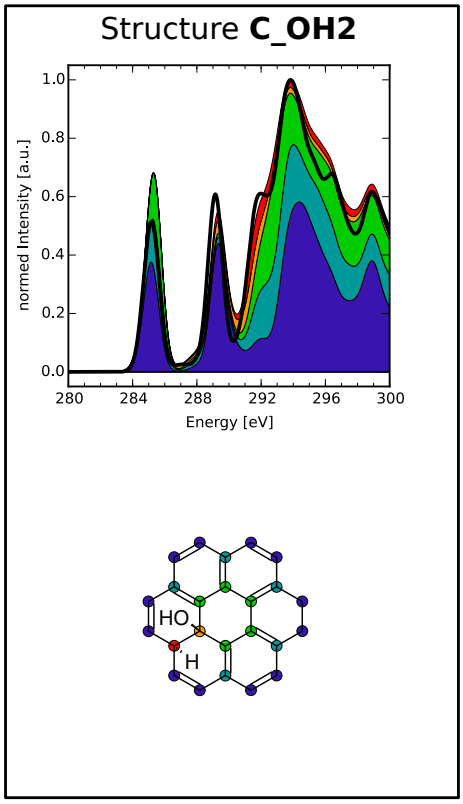
Structure **C_OH2**
normed Intensity [a.u.]
Energy [eV]
HO
H

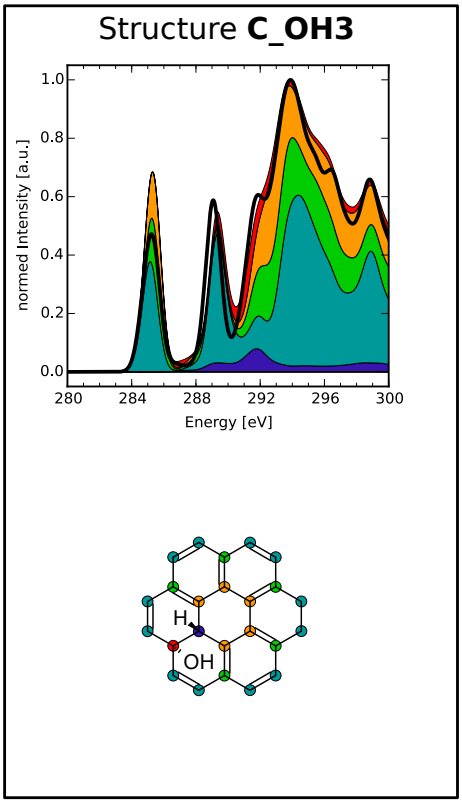
Structure **C_OH3**
normed Intensity [a.u.]
Energy [eV]
H
OH

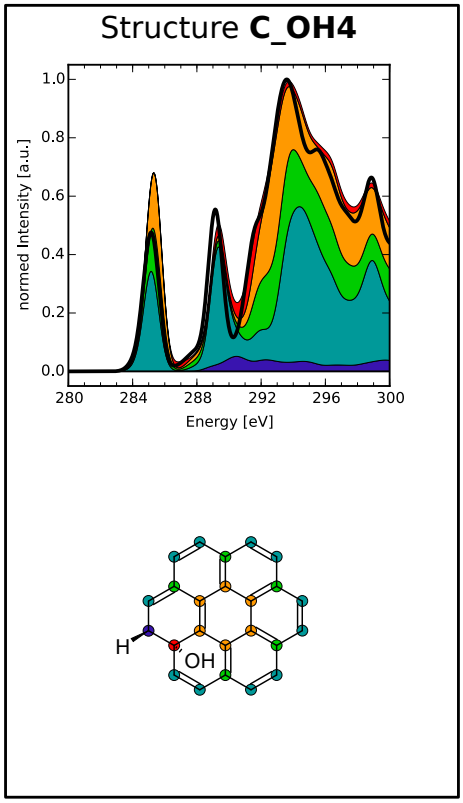
Structure **C_OH4**
normed Intensity [a.u.]
Energy [eV]
H
OH

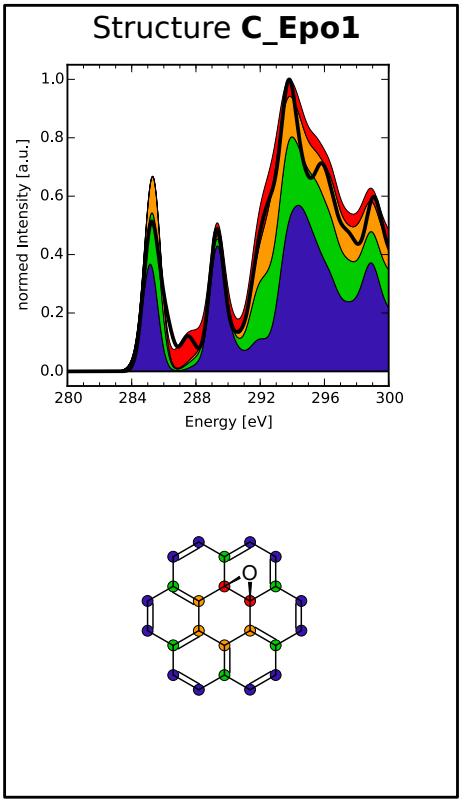
Structure **C_Epo1**
normed Intensity [a.u.]
Energy [eV]
O

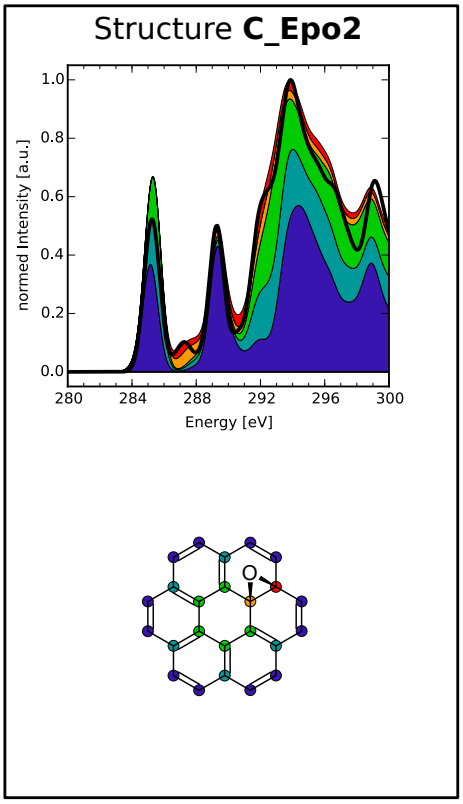
Structure **C_Epo2**
normed Intensity [a.u.]
Energy [eV]
O

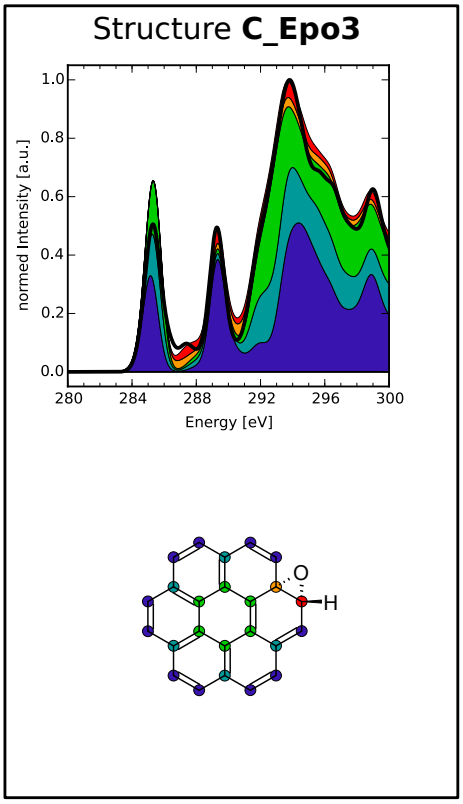
Structure **C_Epo3**
normed Intensity [a.u.]
Energy [eV]
O
H

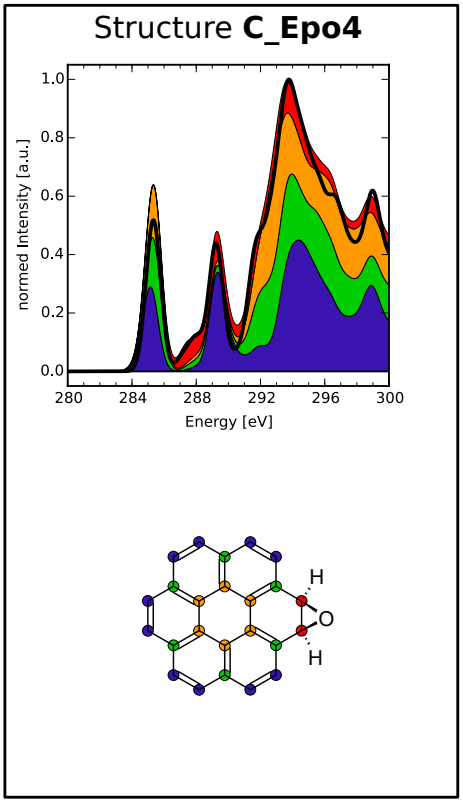
Structure **C_Epo4**
normed Intensity [a.u.]
Energy [eV]
H
O
H

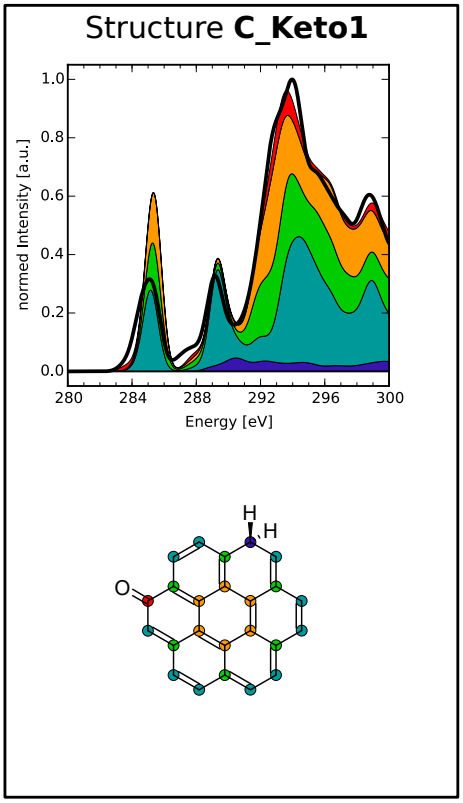
Structure **C_Keto1**
normed Intensity [a.u.]
Energy [eV]
H
H
O

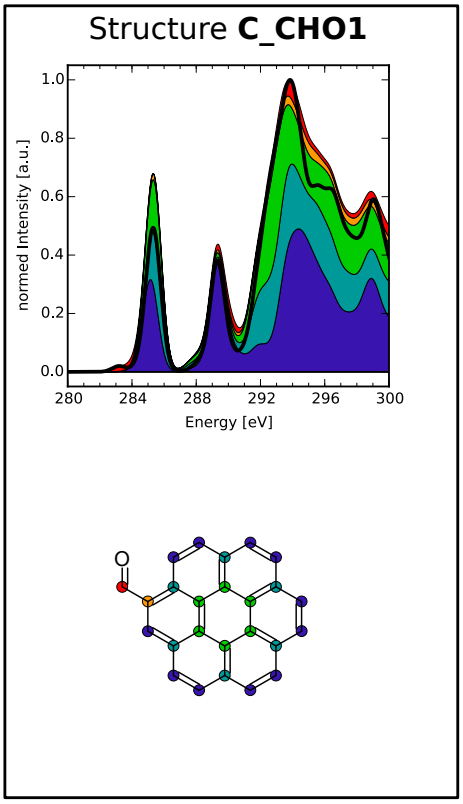
Structure **C_CHO1**
normed Intensity [a.u.]
Energy [eV]
O

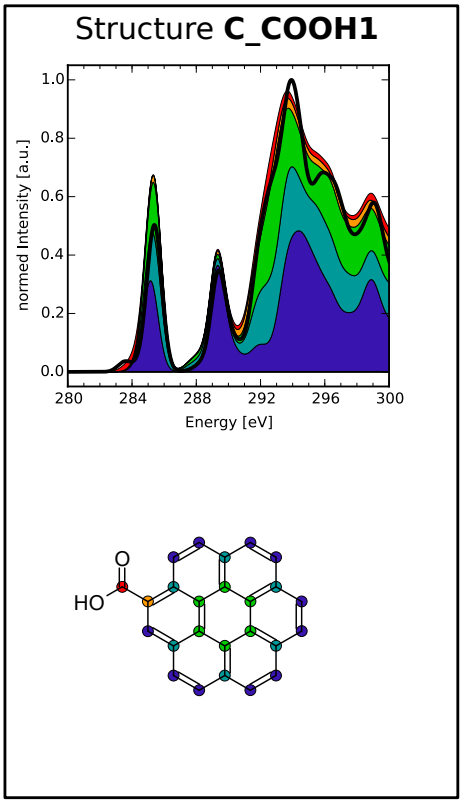
Structure **C_COOH1**
normed Intensity [a.u.]
Energy [eV]
O
HO

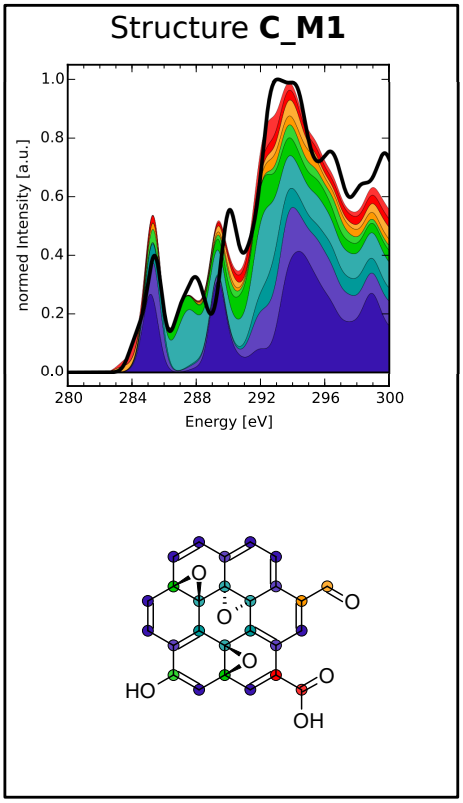
Structure **C_M1**
normed Intensity [a.u.]
Energy [eV]
O
O
O
O
HO
O
OH

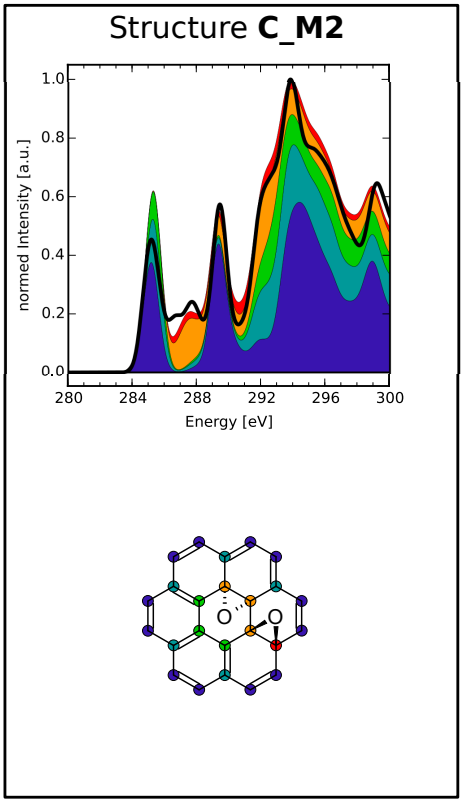
Structure **C_M2**
normed Intensity [a.u.]
Energy [eV]
O
O

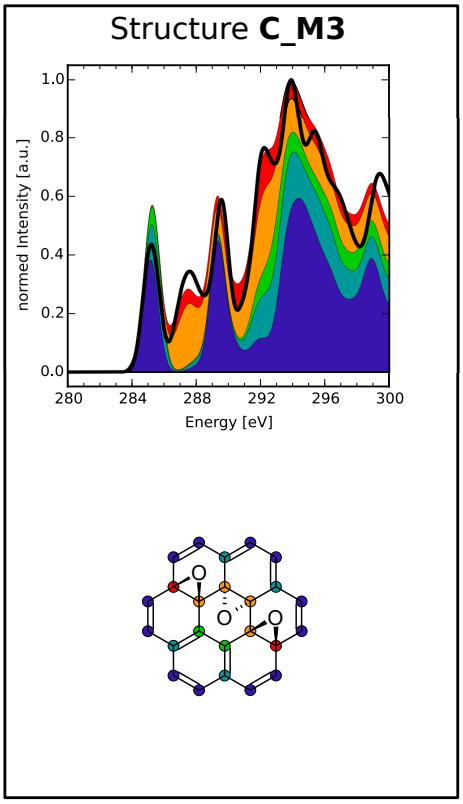
Structure **C_M3**
normed Intensity [a.u.]
Energy [eV]
O
O
O

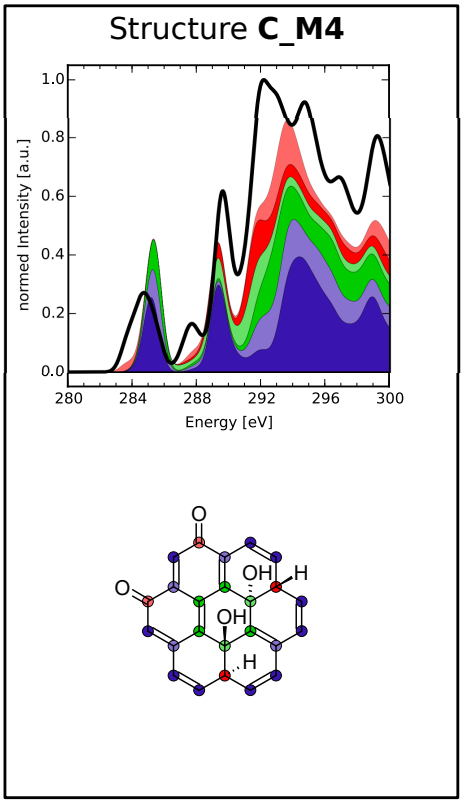
Structure **C_M4**
normed Intensity [a.u.]
Energy [eV]
O
O
OH
H
OH
H

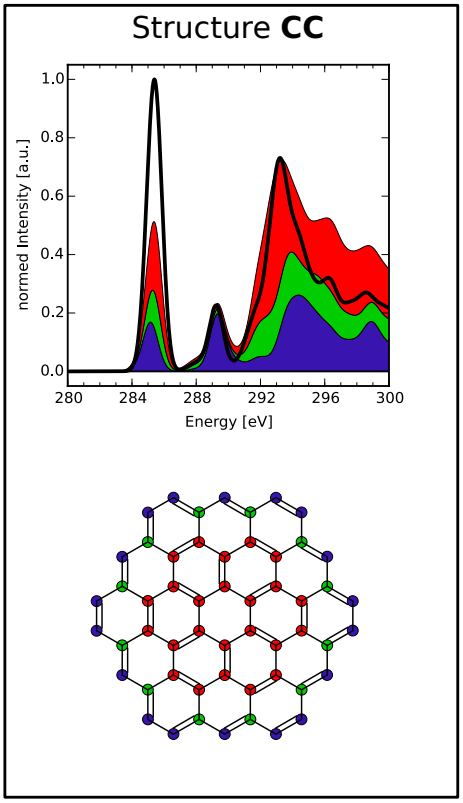
Structure **CC**
normed Intensity [a.u.]
Energy [eV]

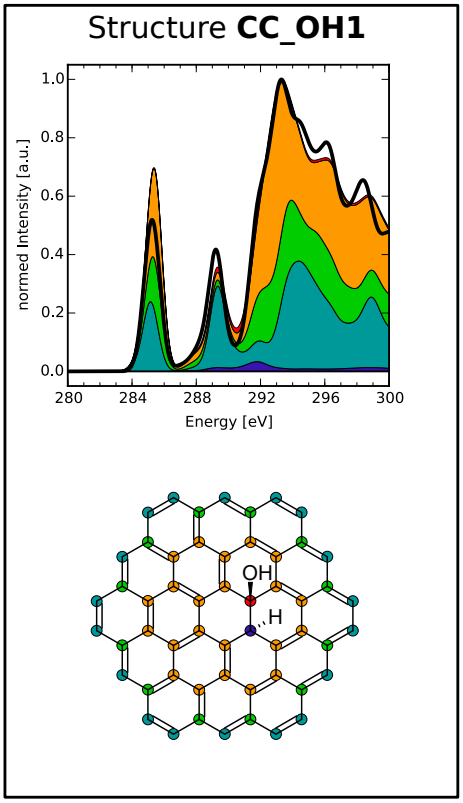
Structure **CC_OH1**
normed Intensity [a.u.]
Energy [eV]
OH
H

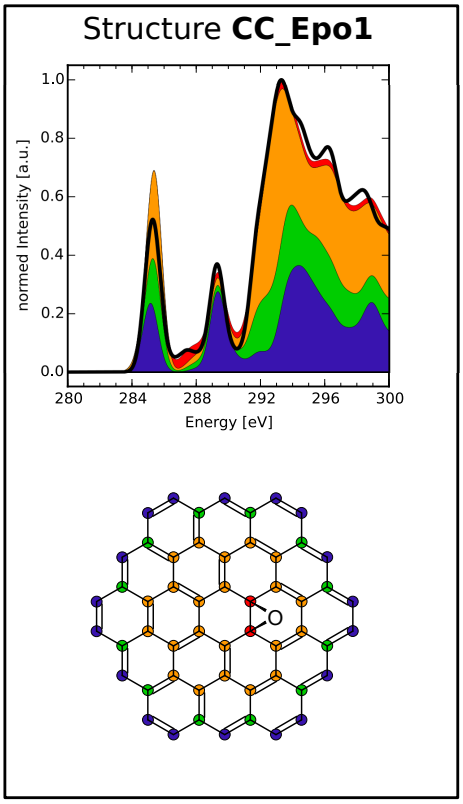
Structure **CC_Epo1**
normed Intensity [a.u.]
Energy [eV]
O

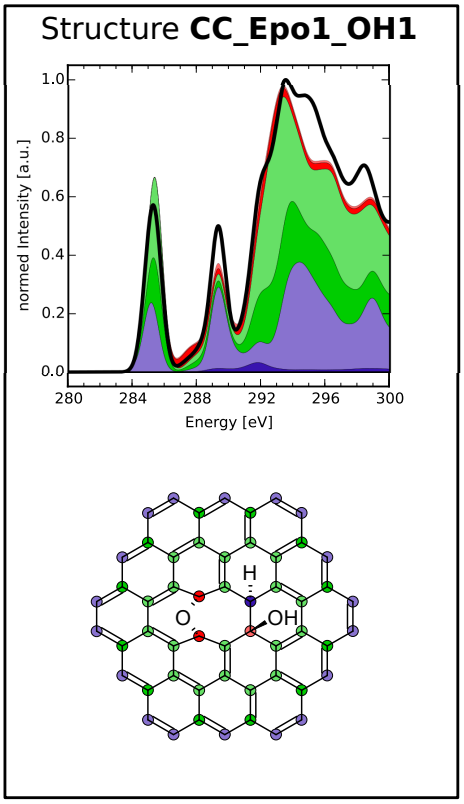
Structure **CC_Epo1_OH1**
normed Intensity [a.u.]
Energy [eV]
H
O
OH

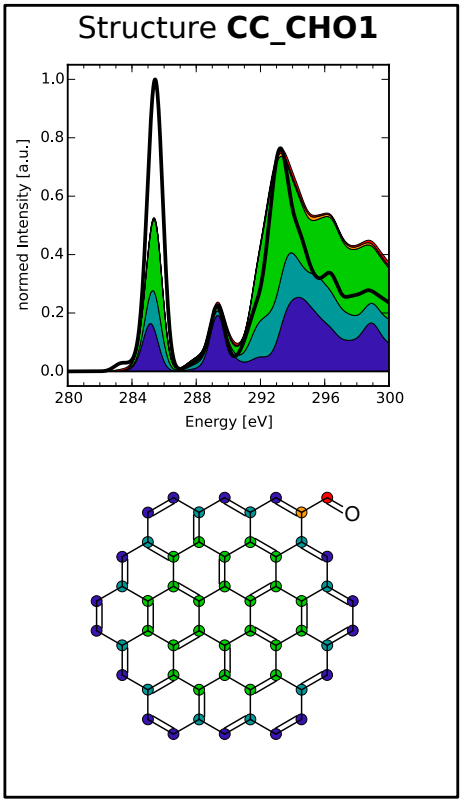
Structure **CC_CHO1**
normed Intensity [a.u.]
Energy [eV]
O

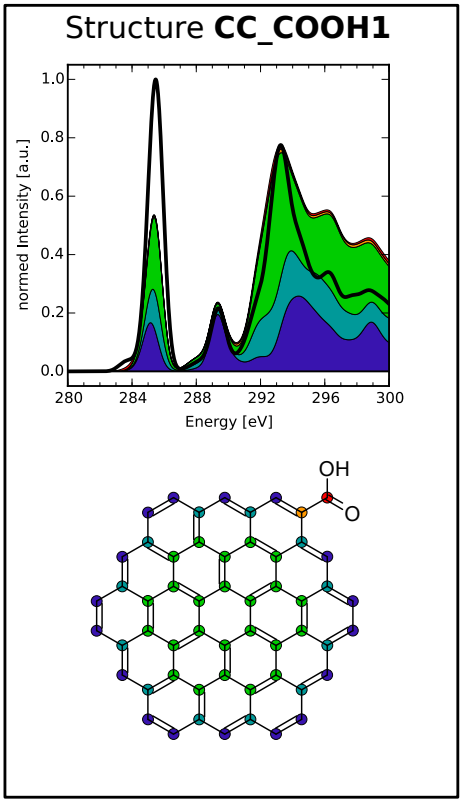
Structure **CC_COOH1**
normed Intensity [a.u.]
Energy [eV]
OH
O

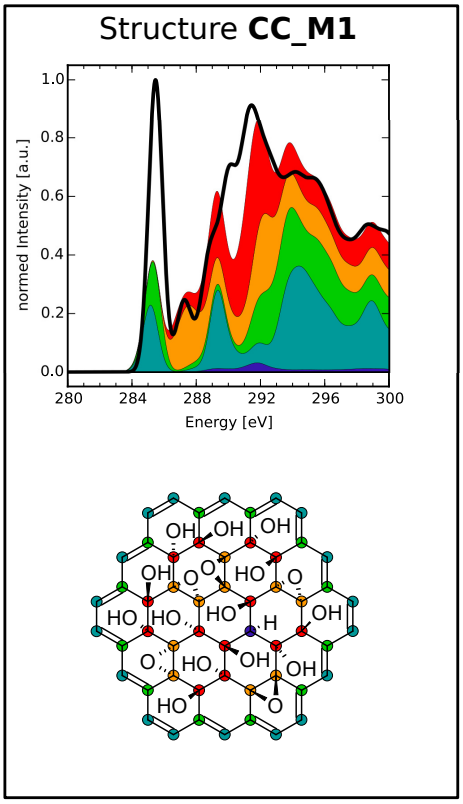
Structure **CC_M1**
normed Intensity [a.u.]
Energy [eV]
OH
HO
O
H

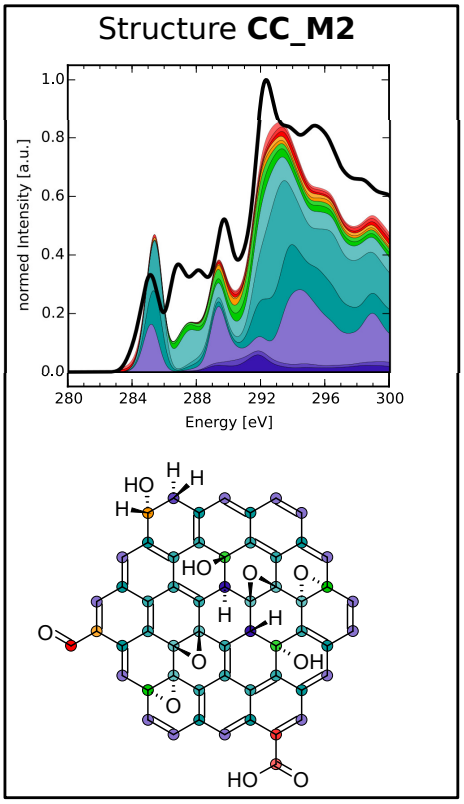
Structure **CC_M2**
normed Intensity [a.u.]
Energy [eV]
HO
H
O
OH

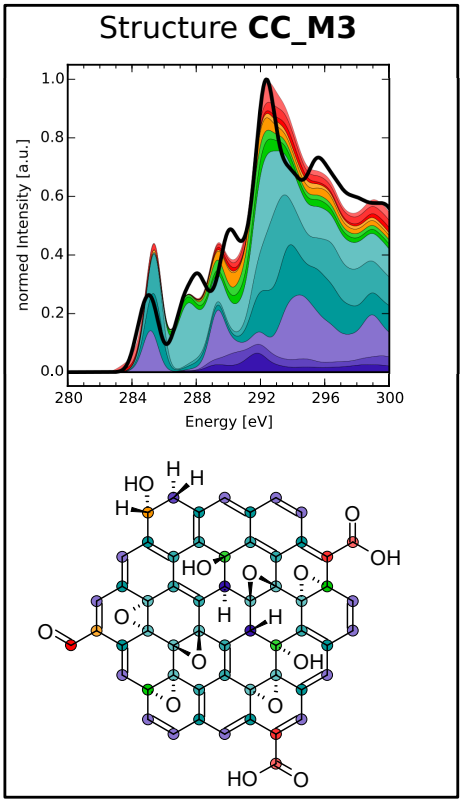
Structure **CC_M3**
normed Intensity [a.u.]
Energy [eV]
HO
H
O
OH

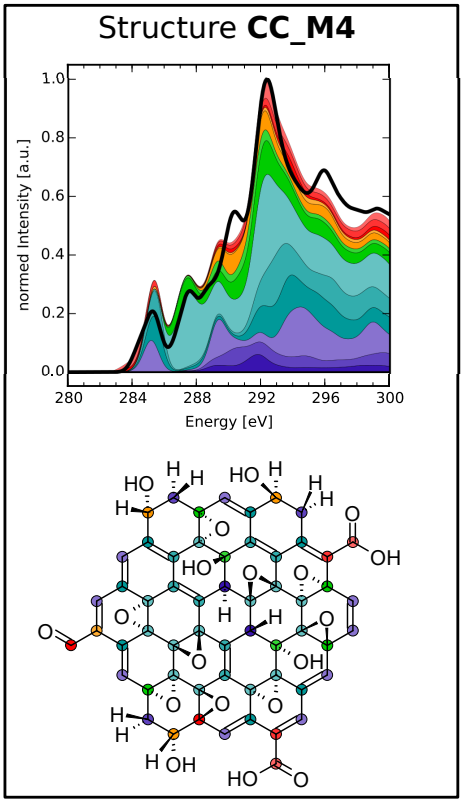
Structure **CC_M4**
normed Intensity [a.u.]
Energy [eV]
HO
H
O
OH

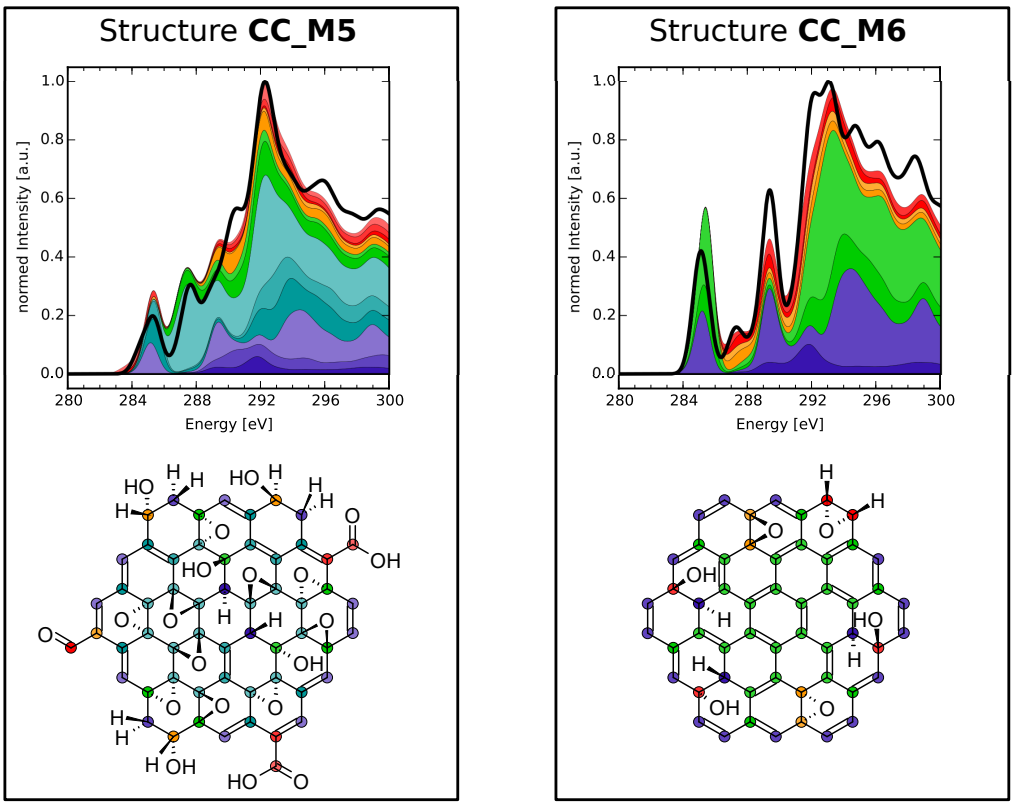

D. FULL SPECTRAL DECOMPOSITION

In the following, the complete experimental spectra of the graphene oxide as well as oxidized carbon dot (CD) samples are shown including their compositions. Note that the analysis can only performed qualitatively beyond the energy of roughly 290 eV, since this is where the ionization continuum begins. To facilitate the understanding of the cumulative sum, we collect the main contributions into four major components. Each of these presents a cumulative sum of different group XA spectra on its own. The exact composition for each of the four components into group XA spectra can be seen in the corresponding panels with all respective weights printed out below. The list of weights is ordered from darker to lighter colors (bottom to top), accordingly.

graphene oxide

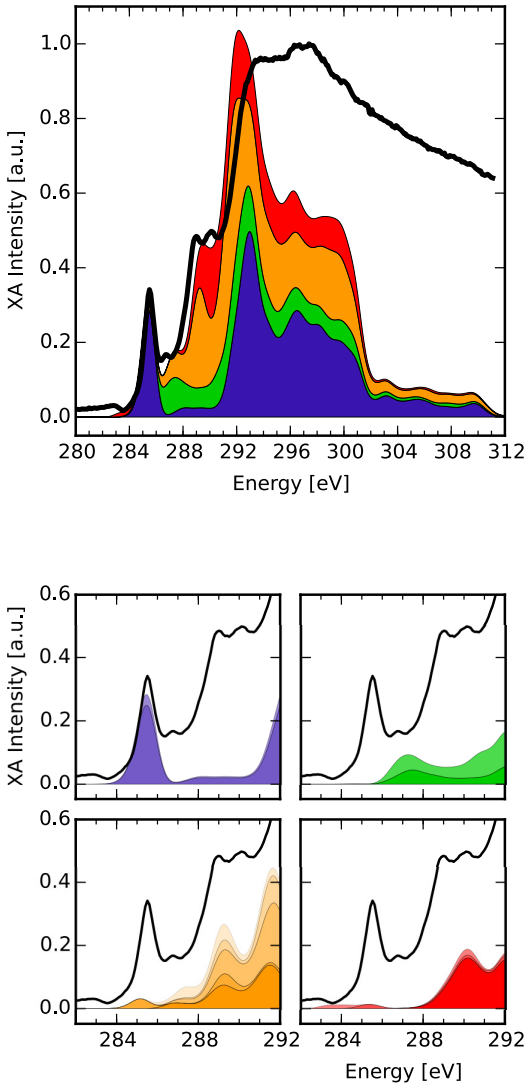

Blue: 0.75 basal C, 0.1 bridge C.
Green: 0.09 basal C-Epo, 0.18 bridge C-Epo.
Orange: 0.175 basal C-OH, 0.1 edge CH, 0.25 basal C-H, 0.1 bridge CH, 0.09 edge CH-Epo.
Red: 0.27 edge CH-OH, 0.06 edge C-CHO, 0.06 CHO.

oxidized CD

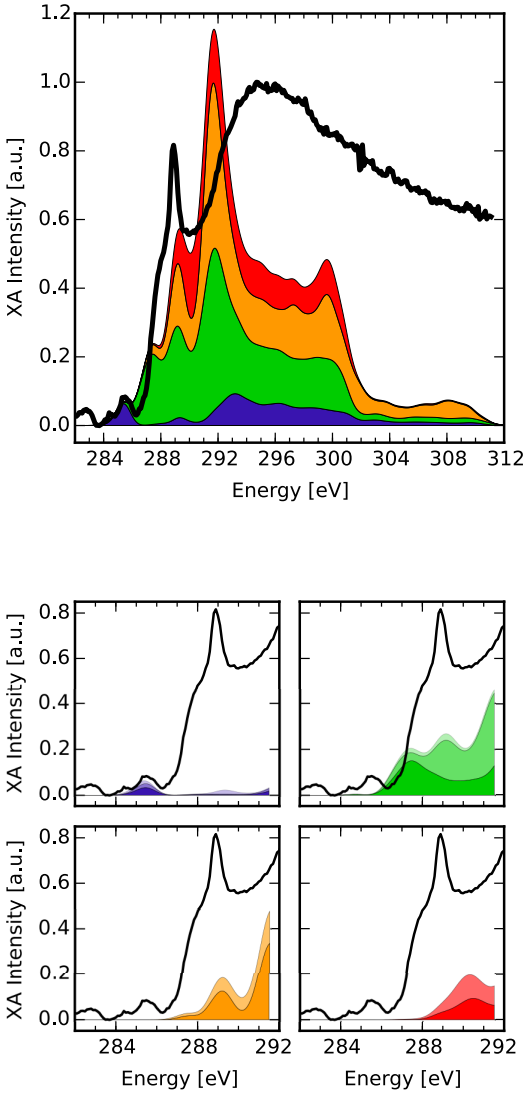

Blue: 0.1 basal C, 0.05 bridge C, 0.05 edge CH.
Green: 0.3 basal C-Epo, 0.4 basal C-OH, 0.05 edge CH-Epo.
Orange: 0.39 bridge CH, 0.195 basal C-H.
Red: 0.18 edge CH_2, 0.18 edge CH-OH.

[1] Ishii, I., Hitchcock, A. P., J. Electron. Spectrosc. Relat. Phenom., **1987**, 46, 55

[2] Gandhiraman, R. P., Nordlund, D., Javier, C., Koehne, J. E., Chen, B., Meyyappan, M., J. Phys. Chem. C, **2014**, 118, 18706

[3] Nikitin, A., Näslund, L.-Å., Zhang, Z., Nilsson, A., Surf. Sci., **2008**, 602, 2575

[4] Knorr, D. B. Jr., Jaye, C., Fischer, D. A., Shoch, A. B., Lenhart, J. L., Langmuir, **2012**, 28, 15294

[5] Urquhart, S. G., Smith, A. P., Ade, H. W., Hitchcock, A. P., Rightor, E. G., Lidy, W., J. Phys. Chem. B, **1999**, 103, 4603

[6] Zhong, J., Zhang, H., Sun, X., Lee, S.-T., Adv. Mater., **2014**, 26, 7786

[7] Sham, T. K., Yang, B. X., Kirz, J., Tse, J. S., Phys. Rev. A, **1989**, 40, 652

[8] Lessard, R., Cuny, J., Cooper, G., Hitchcock, A. P., Chem. Phys., **2007**, 331, 289